
**AFRL-AFOSR-UK-TR-2019-0052**

# Innovative Silicon and InP Integrated Photonic Devices for RF Frequency Downconversion

**Gunther Roelkens**
**UNIVERSITEIT GENT VZW**
**SINT-PIETERSNIEUWSTRAAT 25**
**GENT, 9000**
**BE**

**09/13/2019**
**Final Report**



Air Force Research Laboratory
Air Force Office of Scientific Research
European Office of Aerospace Research and Development
Unit 4515 Box 14, APO AE 09421

# REPORT DOCUMENTATION PAGE

*Form Approved*
*OMB No. 0704-0188*



| 1. REPORT DATE *(DD-MM-YYYY)* | 2. REPORT TYPE | 3. DATES COVERED *(From - To)* |
|---|---|---|
| 13-09-2019 | Final | 14 Dec 2017 to 14 Dec 2018 |

**4. TITLE AND SUBTITLE**
Innovative Silicon and InP Integrated Photonic Devices for RF Frequency Downconversion

**5a. CONTRACT NUMBER**

**5b. GRANT NUMBER**
FA9550-18-1-0015

**5c. PROGRAM ELEMENT NUMBER**
61102F

**6. AUTHOR(S)**
Gunther Roelkens

**5d. PROJECT NUMBER**

**5e. TASK NUMBER**

**5f. WORK UNIT NUMBER**

**7. PERFORMING ORGANIZATION NAME(S) AND ADDRESS(ES)**
UNIVERSITEIT GENT VZW
SINT-PIETERSNIEUWSTRAAT 25
GENT, 9000 BE

**8. PERFORMING ORGANIZATION REPORT NUMBER**

**9. SPONSORING/MONITORING AGENCY NAME(S) AND ADDRESS(ES)**
EOARD
Unit 4515
APO AE 09421-4515

**10. SPONSOR/MONITOR'S ACRONYM(S)**
AFRL/AFOSR IOE

**11. SPONSOR/MONITOR'S REPORT NUMBER(S)**
AFRL-AFOSR-UK-TR-2019-0052

**12. DISTRIBUTION/AVAILABILITY STATEMENT**
A DISTRIBUTION UNLIMITED: PB Public Release

**13. SUPPLEMENTARY NOTES**

**14. ABSTRACT**

We demonstrated that two monolithically integrated InP-based lasers integrated on a single chip can be locked to the same optical cavity using the PDH frequency locking technique. The PDH is implemented with a single control loop and voltage control electro-optic tuning therefore avoiding significant heat dissipation. The frequency difference of the stabilized lasers can be discretely tuned at multiples of the FSR of the external optical cavity and used for RF signal generation. We presented generated tones at 12.436 GHz, 24.8735 GHz and 40.4194 GHz, limited only by the bandwidth of the photodetector, with FWHM <40 kHz. The SSB phase noise is lower than 50 dBc/Hz for all frequency offsets.
The obtained SSB phase noise of the RF signal is not as good as state of the art oscillators up to several tens of GHz frequency at the moment. The phase noise can be improved however in two ways. At low offset frequencies (couple of MHz) further suppression of the laser frequency noise can be achieved with improvement of the PDH locking system with higher gain. At high offset frequencies, lasers with lower intrinsic linewidth should be used since implementation of PDH locking with such control bandwidths is very challenging.
Despite the SSB phase noise not being better than the state-of-the-art this technique has several advantages. The tuning range can be extended by more than an order of magnitude by using lasers realised in the same technology. Such tuneable lasers can be tuned over tens of nm (several THz) and can be stabilized in the same way as shown in this report. Therefore discrete tuning from microwave to THz frequencies can be enabled. In the same technology we have demonstrated that widely tuneable lasers can have roughly the same frequency noise level independent of their lasing wavelength. The implementation of this technique with such lasers would yield virtually qua

**15. SUBJECT TERMS**
silicon photonic integration, integrated microwave photonics, RF frequency downconversion

| 16. SECURITY CLASSIFICATION OF: | | | 17. LIMITATION OF ABSTRACT | 18. NUMBER OF PAGES | 19a. NAME OF RESPONSIBLE PERSON |
|---|---|---|---|---|---|
| a. REPORT | b. ABSTRACT | c. THIS PAGE | | | LOCKWOOD, NATHANIEL |
| Unclassified | Unclassified | Unclassified | SAR | | 19b. TELEPHONE NUMBER *(Include area code)* 011-44-1895-616005 |

Standard Form 298 (Rev. 8/98)
Prescribed by ANSI Std. Z39.18

# Innovative Silicon and InP integrated photonic devices for RF Frequency downconversion (FA9550-18-1-0015)

**Kasper Van Gasse, *Gunther Roelkens***
*Photonics Research Group, Ghent University – imec, 9052 Ghent, Belgium*
*e-mail: kasper.vangasse@ugent.be, gunther.roelkens@ugent.be*

**Stefanos Andreou, *Erwin A. J. M. Bente***
*Institute for Photonic Integration, Eindhoven University of Technology, P.O. Box 513 – 5600 MB, Eindhoven, The Netherlands*
*e-mail: s.andreou@tue.nl, e.a.j.m.bente@tue.nl*

**ABSTRACT**
We demonstrate the generation of radio-frequency (RF) signals using stabilized integrated semiconductor lasers. The lasers are monolithically integrated on the same chip using InP active-passive integration technology. They are locked to different resonances of the same external optical cavity using the Pound-Drever-Hall locking technique. The locking is implement with a single control loop for each laser and by voltage controlled tuning thus avoiding significant thermal effects. The generated RF signal can be tuned discretely to frequencies that are multiples of the external optical cavity free spectral range. Examples of beat tones at 12.436, 24.8735 and 40.4194 GHz are demonstrated. The linewidth of the generated signals at all frequencies is less than 40 kHz. The single-side-band phase noise is about -54 dBc/Hz for frequencies offsets from the carrier at 12.436 GHz between 1 kHz and 10 kHz and -60 and -67 dBc/Hz at 100 kHz and 1 MHz respectively.We also demonstrate the realization of silicon photonics-based RF modulators. Optimized structures are designed and realized for 30 GHz operation, including a resonant Si Mach-Zehnder modulator and a traveling wave Mach-Zehnder modulator.

## 1. PHOTONICS-BASED MICROWAVE SOURCES

High quality oscillators with wide tuneability in the radio-frequency (RF) and millimetre-wave range are key components in radar systems, high data rate wireless communications, in the transportation of signals over very long distances and instrumentation. Generation of such signals is commonly implemented by leveraging mature electronic technologies which are widely available. In the context of microwave photonics, generation of RF signals has been demonstrated by utilizing photonic technologies as well [1]. The advantages of photonic techniques include: the generation of signals in a wider range from RF to THz frequencies, a wide tuneability, and the distribution of signals with low propagation loss through fibres instead of coaxial cables.

Several techniques are available for down-conversion from the near-infrared wavelength region (optical domain) to RF/millimetre-wave and/or THz frequencies. The simplest method is the heterodyne method [2], realised by mixing two single mode lasers on a photodetector with sufficient bandwidth. More heterodyne schemes that additionally involve electrical feedback and/or optical injection [3] and different approaches such as frequency combs [4] and opto-electronic oscillators [5] have also been demonstrated.

Here we focus on the heterodyne method which is implemented by heterodyning two frequency stabilized integrated lasers. The deployed lasers are monolithically integrated on a single chip using InP

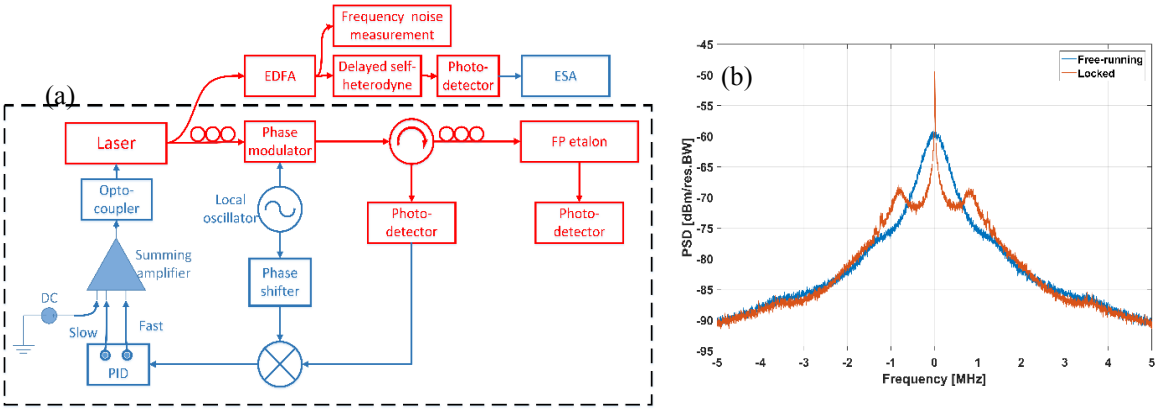


*Fig. 1 (a) Schematic of used PDH locking of an integrated laser with a single feedback loop, (b) Electrical spectra measured with the delayed self-heterodyne method for the free-running (blue) and locked (orange) laser. The locked laser shows a linewidth of ~5 kHz compared to the free-running that exhibits a linewidth of ~300 kHz mainly determined by technical noise.*

active-passive integration technology [6]. The frequency of each laser is locked on an optical resonance of the same external optical cavity, a highly stable Fabry-Perot etalon. The locking at different optical resonances is done using the Pound-Drever-Hall (PDH) frequency locking technique [7]. The single electrical feedback electro-optically tunes the laser with a reverse bias voltage. The frequency difference of the two lasers can be discretely tuned at multiples of the free-spectra range (FSR) of the optical cavity. The RF signal is generated by an external high-speed photodetector. In the first section we present results on the PDH stabilization of a single frequency integrated laser. The locking is performed using a single feedback loop and deploying a voltage-controlled intra-cavity phase modulator for tuning. In the second section we explain in more detail the RF signal generation scheme with the two stabilized lasers. In the third part examples of the RF signals at 12, 24 and 40 GHz are shown.

### 1.1. POUND-DREVER-HALL STABILIZATION OF InP-BASED INTEGRATED LASERS

In this section we briefly present the stabilization of integrated diode lasers which were used for the RF signal generation. The lasers were fabricated by Smart Photonics [6] in a multi-project wafer run using a commercially available InP-based active-passive integration technology. The lasers are multi-section distributed Bragg reflector (DBR) lasers with an intra-cavity ring resonator lasing at 1540 nm. More details on the laser can be found in [8]. In this technology, the lasing wavelength can be tuned by reverse biasing the DBR mirrors and/or phase sections in the laser cavity. This reverse bias phase control is based primarily on electro-optic effects with no significant thermal effects. The negative electrical feedback used in the PDH technique is also applied as a reverse bias voltage on the DBR mirror section. This is in contrast with the more often used current feedback which relies on current density changes and thermal effects which have an opposite effect on the laser frequency. A single feedback loop combining both low- and high-bandwidth outputs of the PID controller loop is used in this case.

In Fig. 1(a) the schematic of the PDH locking used is presented. The chip on which the laser is integrated is temperature controlled at 18 °C using a watercooler. The laser output is directed to the chip facets with an angled waveguide to avoid back-reflections. The facet is anti-reflection coated. Light is collected using a single-mode lensed fibre. The phase modulation frequency used for the PDH locking is 60 MHz and the optical reference cavity is a temperature stabilised Fabry-Perot etalon with a full-width at half-maximum of ~0.7 MHz of the resonance peak and ~3.125 GHz free spectral range (FSR). An average of 20 measurements of the laser linewidth using a delayed self-heterodyne setup with a 25 km delay line is shown in Fig. 1(b). The free-running laser (blue trace) exhibits a Gaussian lineshape with a laser linewidth of about 300 kHz, mainly determined by technical noise. The locked laser (orange) in the same figure exhibits a linewidth of about 5 kHz. The gain bandwidth of the control loop is about 500 kHz. The side-peaks around 800 kHz offset in the spectrum are due to the phase lag of the control

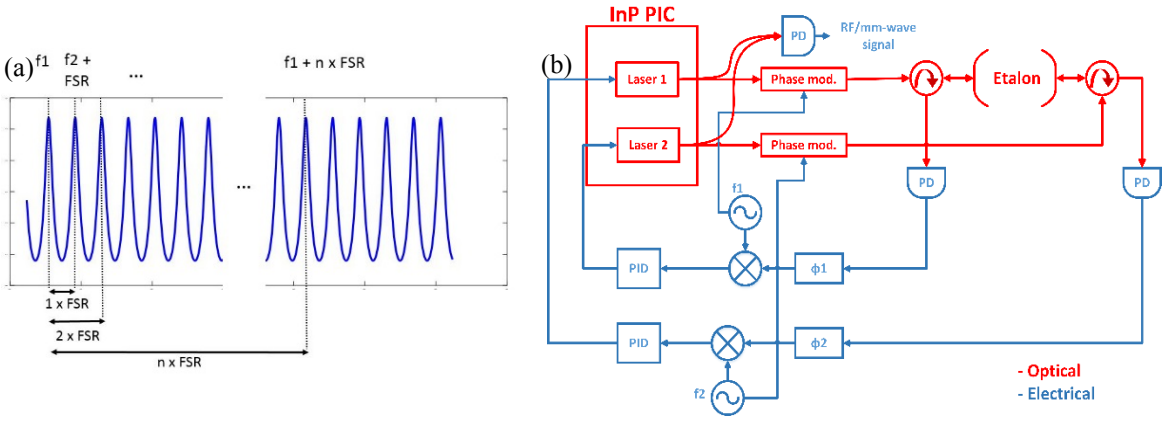


*Fig. 2 (a) Principle of dual-mode Pound-Drever-Hall stabilization. Two lasers can be locked to two different longitudinal modes of a cavity therefore discrete tuning of the RF signal is possible at multiples of the cavity FSR, (b) Schematic of the dual-mode PDH stabilization. The two lasers are locked on the same Fabry-Perot cavity but at different resonances. The modulation frequency for each laser is also different in order to avoid interference.*

loop. The linewidth of the locked laser is reduced more than 1/100 of the optical cavity FWHM. Its long-term stability is identical to the stability of the cavity.

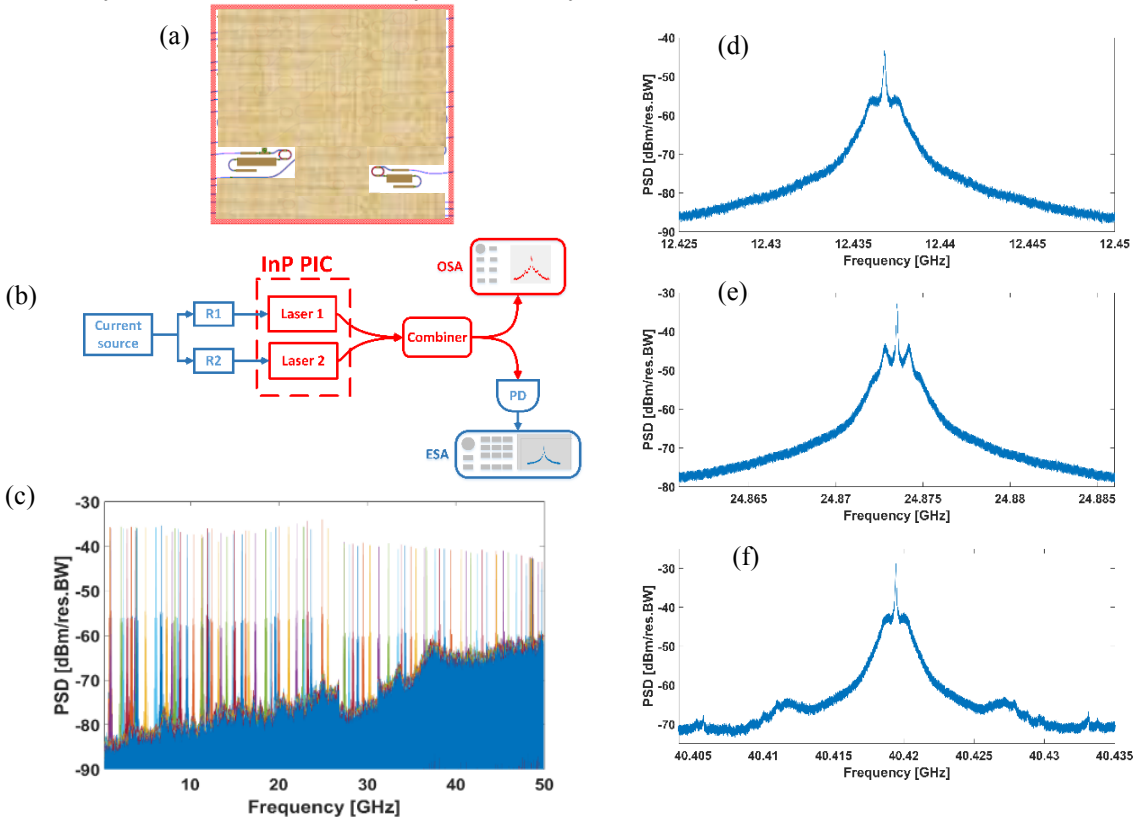


*Fig. 3 (a) Two monolithically integrated single mode lasers on a single chip, (b) experimental setup showing how the lasers are tuned and (c) their continuously tuned frequency difference of the free-running lasers over 50 GHz. (d), (e) and (f) the RF tones generated at 12.436 GHz, 24.8735 GHz and 40.4194 GHz by mixing the two locked lasers on a high-speed photodetector. The lasers are locked to resonance which are 3, 8 and 13 FSRs apart from each other.*

## 1.2. STABILIZATION OF INTEGRATED LASERS TO A SINGLE OPTICAL CAVITY

The periodic transmission spectrum of a Fabry-Perot etalon is shown schematically in Fig. 2(a). Two lasers can be locked to different resonances of the cavity, spaced by *n* x FSR, where FSR is the FSR range of the cavity and *n* is an integer. In Fig. 2(b) a schematic of the stabilization of two integrated

lasers to the two different cavity modes using the PDH locking is shown. The phase modulated output of the two lasers fall onto the optical cavity, one on each of the two mirrors. The two phase modulation frequencies are slightly different, 55 and 60 MHz, in order to avoid interference after the down-conversion. The error signal of one laser is not down-converted to DC at the mixer output of the other laser but to the frequency difference of the two modulation frequencies. The control loops of the two lasers are otherwise identical. The polarization of the light falling onto the cavity is also the same for the two lasers. The tones in the RF domain are generated by mixing the two locked lasers on a 50 GHz photodetector.

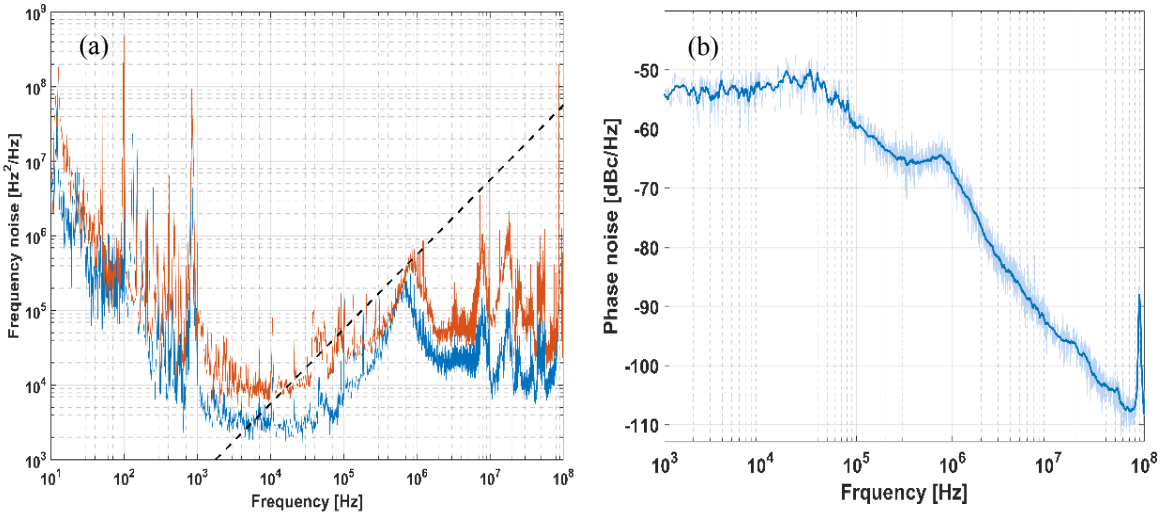


*Figure 4 (a) Frequency noise of the two locked lasers used for the RF signal generation at 12.43 GHz, (b) SSB phase noise of RF tone at 12.43 GHz.*

The phase noise of the resulting RF signal is a combination of two aspects. The first is the quality of the laser locking. The locking reduces the technical noise and intrinsic noise in the laser frequency at low frequencies where the control loop gain is effective. In our case the control loop has a bandwidth of about 500 kHz as discussed in section 2. The second is the laser white part of the frequency noise defined by the laser amplified spontaneous emission. The white noise is dominant at frequencies higher than the control loop bandwidth where technical noise is also not present. Moreover, the phase noise characteristics of the generated tones should be independent of their frequency. This is a valid assumption because the laser linewidth does not significantly differ over the tuning range of the lasers. This is true for semiconductor lasers in general. The long-term stability of the generated tone and its central frequency is defined by the length stability of the optical cavity on which the lasers are locked. Any changes in length due to vibrations or thermal effects should in first order approximation affect the two locked lasers in the same way. The cavity FSR should undergo much smaller changes.

### 1.3. RF SIGNAL GENERATION RESULTS

The two lasers used have the same cavity design as the laser presented in section 2. They are monolithically integrated on the same chip (Fig. 3(a)). Both lasers are operated by the same current source and the current is distributed to the lasers using a current divider network with two potentiometers (Fig. 3(b)). The maximum value of the two series resistances is 50 Ω. This resistance value is about 6 to 7 times larger than the series resistance of the laser's SOAs which contributes to the 1/f noise of the lasers. We keep the total injected current constant and we change only the current ratio of the two branches. The two lasers and their frequency difference are tuned only by their SOA current through thermal tuning. We monitor the output of the two lasers using an optical spectrum analyser and an electrical spectrum analyser after beating them on the 50 GHz photodetector. In Fig. 3(c) we show that we can continuously tune the difference for at least 50 GHz, limited by the photodetector bandwidth. The RF power is relatively constant since the lasers are operated in the linear region of their light-current curve.

We have locked the two lasers on resonances with different spacing. In Fig. 3(d), (e) and (f) three examples are presented with tones at 12.436 GHz, 24.8735 GHz and 40.4194 GHz respectively. These frequencies correspond to 4, 8 and 13 FSRs. The effect of the frequency locking on the RF tone lineshape

is visible as in Fig. 1(b). The noise around the RF tone is supressed up to the frequency offset where the control loop runs out of bandwidth. The effect of the locking system in the three cases is slightly different as can be seen from the side-peaks caused by the bandwidth roll-off. This is attributed to small differences of the PID parameters used. In these three cases we obtain a FWHM of the RF tone of 40 kHz, 35 kHz and 30 kHz at 12.436 GHz, 24.8735 GHz and 40.4194 GHz respectively.

The frequency noise of the locked lasers that were used for generating the 12.436 GHz tone was measured and it is presented in Fig. 4(a). Their frequency noise and therefore contribution to single-side band (SSB) phase noise of the RF signal (Fig. 4(b)) is slightly different. Nevertheless, both lasers exhibit qualitatively the same behaviour. Noise is supressed more effectively in the frequency range from 1 kHz to 200 kHz. Below this range several spurious peaks appear which degrade the locking quality and above it the control loop is no longer effective. The origin of the peak at 950 Hz is unknown but we suspect it originates from the electronics. The wide peak at ~800 kHz is due to the phase lag of the control loop. A more detailed image of the quality of the generated signal at 12.436 GHz is presented in Fig. 4(b). The SSB phase noise is about -53 dBc/Hz from 1 kHz to 10 kHz offset from the carrier. Then it drops to -60, -67 and -93 dBc/Hz at 100 kHz, 1 MHz and 10 MHz respectively. The effect of the control loop is also visible up to about ~1 MHz. In fact the phase noise is slightly increased at 0.8 MHz due to the control loop phase lag which is also visible in the laser frequency noise.

## 2. SILICON PHOTONICS RF MODULATORS FOR 30 GHZ OPERATION

In this section we present the design, fabrication and characterization of two silicon photonic modulators. We designed and characterized a silicon carrier-depletion dual-parallel Mach-Zehnder modulator that can be used for microwave photonic applications such as microwave photonic frequency conversion. As microwave systems often operate in a 50 Ohm environment, we investigated advanced electrode design to provide on-chip impedance matching without the use of resistive elements. Stub-matching electrodes were designed and characterized.

Over the last years a great amount of research has been dedicated to the development of high-bandwidth optical modulators on integrated photonic platforms, such as silicon photonics, InP photonics and hybrid InP/Si photonics. Mach-Zehnder Modulators (MZMs) based on pn-doped silicon waveguide phase-shifters have seen tremendous progress in recent years. Although both carrier-injection and carrier-depletion phase-shifters have been investigated, carrier-depletion has shown great promise for high-bandwidth applications. Furthermore, IQ-modulators can be implemented by placing two parallel MZMs in a Mach-Zehnder Interferometer (MZI) structure. Such modulators are also referred to as dual-parallel MZMs and they can be used for complex modulation formats used in coherent communication. The use of dual-parallel MZMs is also of great interest to the microwave photonics community, as they can be used for microwave photonic frequency conversion and single-sideband modulation. Especially in Radio-over-Fiber links single-sideband modulation can be of great interest to mitigate fiber-dispersion induced fading. For digital communication, broadband matching is needed to ensure minimal distortion of the modulated signal. Silicon photonic modulators for digital data transmission often use a travelling-wave electrode in combination with an on-chip 50 Ohm termination to achieve wide-band impedance matching. Although this is an effective approach, the use of resistive impedance matching also has drawbacks. For example, the static bias needed for proper operation of a carrier-depletion phase-shifter will cause constant power dissipation in the 50 Ohm termination. For narrow band applications, such as Radio-over-Fiber, broad-band matching is not needed and non-resistive matching can be used. For example, stub-matching can be used for narrow-band matching of phase-shifter electrodes. The use of stub-matching for optical modulators was already explored for $LiNbO_3$ and promising narrow-band performance was demonstrated. We implemented several designs using an iSiPP25G Multi-Project Wafer run, provided by imec. The photonic technology developed by imec was oriented towards 25~Gb/s data transmission and was therefore called iSiPP25G. We used this technology to develop a dual-parallel MZM capable of microwave photonic frequency conversion. Furthermore, we designed and tested a narrow-band stub-matched phase shifter.

### 2.1. TRAVELING WAVE IQ MODULATOR

We developed a silicon photonic dual-parallel MZM using the iSiPP25G carrier-depletion phase-shifters. The design of the individual MZMs is based on the push-pull design reported in [9]. A schematic layout of the design is shown in Figure 5.

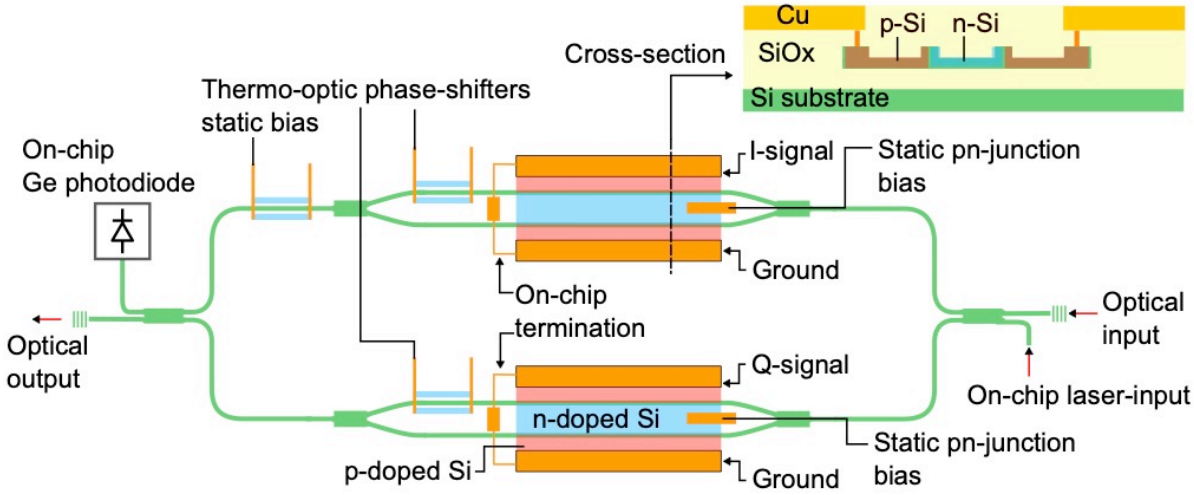


*Figure 5. Schematic of the traveling wave Mach-Zehnder modulator*

In this layout the different components are denoted together with a cross-section of the phase-shifting waveguides. In this design two pn-doped waveguides are placed closely together and driven using a single travelling wave electrode. The pn-doped waveguides from the iSiPP25G PDK have a voltage-length product of approximately 1 Vcm and an optical loss of 3 dB/mm. Given that the effective length of the phase-shifter is 1 mm, the resulting Vpi is approximately 10 V and the insertion loss due to the doped waveguides is approximately 3dB. By electrically connecting the n-doped regions of the two phase-shifters the capacitances of the depletion regions are connected in series. This reduces the capacitance and the microwave propagation losses. A fabrication layout (gds file) of the modulator and a simplified equivalent electrical circuit are shown in Figure 6.

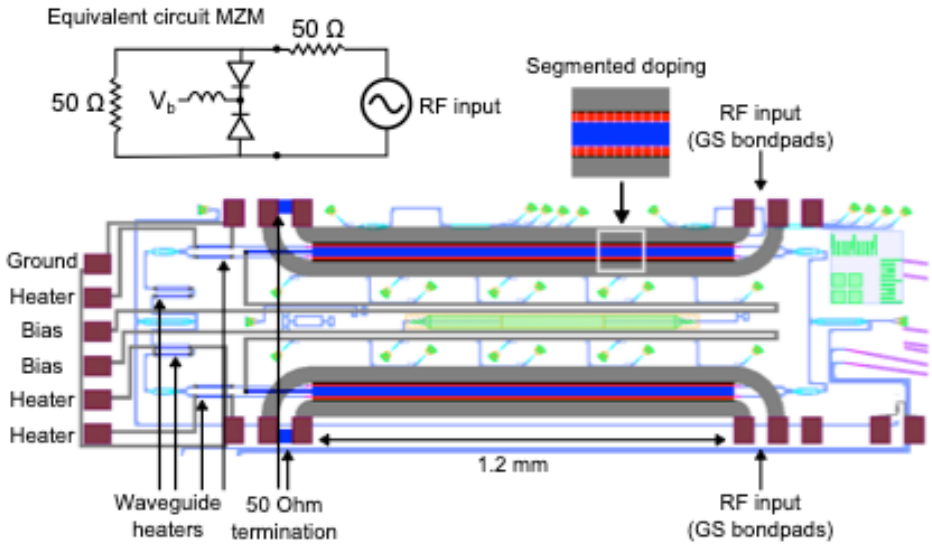


*Figure 6: GDS of the designed traveling wave Mach-Zehnder modulator and an equivalent electrical circuit for the push pull operation. The inset shows the segmented doping profile applied.*

The doping was segmented to reduce possible parasitic transmission line losses as shown in the inset of Figure 6. The optical structure of the MZMs and the MZI were realized using 2 by 2 MMIs. A thermo-

optic phase shifter was added to each individual MZM and the MZI structure. These extra phase shifters are used to provide a static bias to the MZMs and MZI that is needed for IQ-modulation. This is necessary because in the push-pull configuration it is inefficient to provide each pn-junction with an individual static bias. An on-chip 50 Ohm resistor was added to terminate the transmission line electrodes to avoid unwanted reflections and excessive ripple in the modulation response. To provide a static bias on the pn-junctions a separate biasing contact is implemented using a long metal trace, that acts as an RF choke. This way a static bias can be provided without drawing current through the 50 Ohm resistor. The high-frequency inputs for the modulators are on opposite sides of the chip so that they can be easily contacted with RF probes. Chip-to-fiber grating couplers were used for optical I/O using a cleaved single-mode fiber. A microscope image of the fabricated PIC is shown in Figure 7.

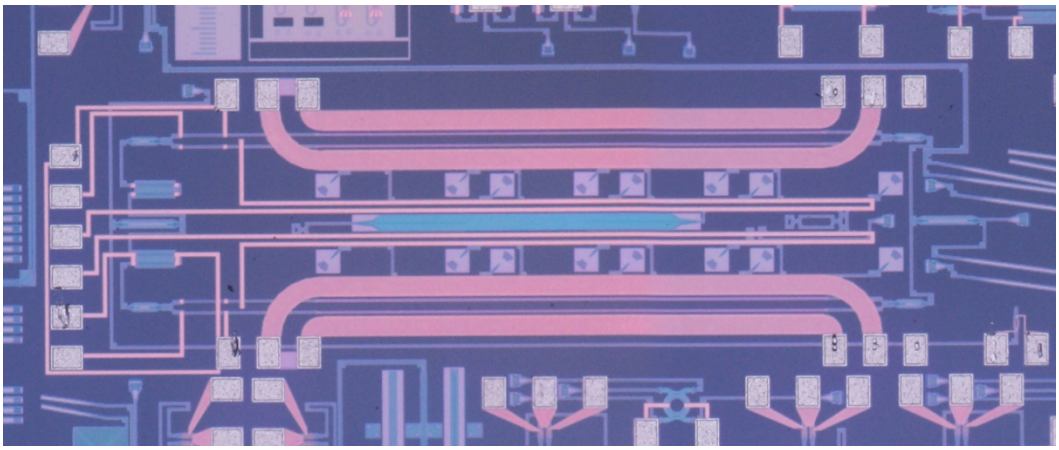

*Figure 7 Microscope picture of the realized traveling wave MZM*

To assess the performance of the individual modulators a small-signal measurement was performed using a Keysight PNA-X Vector Network Analyzer. It was found that the modulation shows less than 3 dB ripple up to 30 GHz. The measured small-signal modulation response, for different bias-voltages across the pn-junction, is shown in Figure 8.

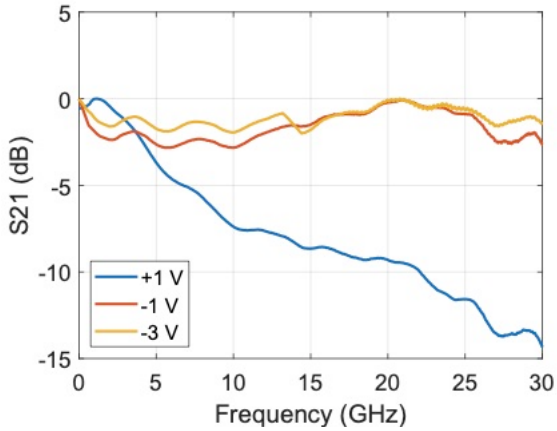


*Figure 8: S21 of the modulator as a function of reverse bias. 30 GHz bandwidth is obtained under reverse bias*

## 2.2. STUB-MATCHED STRUCTURE

As discussed in the previous section, narrow-band impedance matching can be achieved avoiding the use of on-chip resistors. This is interesting as resistive matching dissipates power when compared to pure reactive matching. For example, stub-matching can provide low-loss narrow-band impedance matching. Stubs are short pieces of transmission line which are connected on one side to the feed transmission line. The use of stubs is a well-known matching technique used in microwave and RF

engineering. The use of stub-matching has been previously demonstrated for narrow-band impedance matching of resonant LiNbO3 electrodes.
With this approach excellent matching was achieved for frequencies higher than 20 GHz. However, to the best of our knowledge this approach has never been implemented in silicon photonics. The imec iSiPP25G platform offers a metal layer (Cu damascene) which allows for the design of microwave transmission lines. This allowed to implement a phase shifter electrode with on-chip stub-matching. Based on the designs previously reported in [10] and [11] we chose to develop a phase-shifter with open-ended electrode and open-ended stubs connected at the feed point. A schematic layout of the implementation of such a modulator on the iSiPP25G platform is shown in Figure 9.

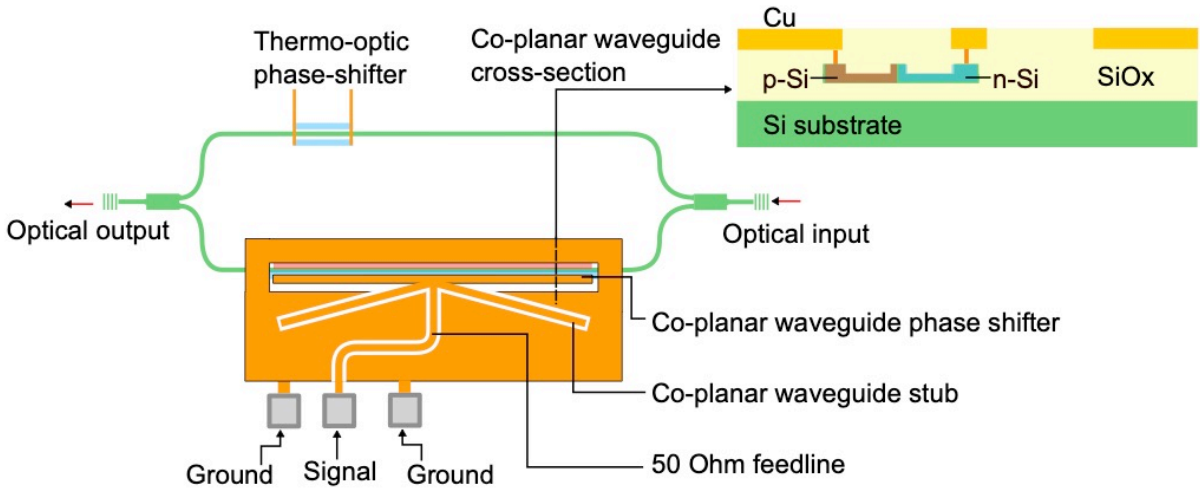


*Figure 9 Schematic of the resonant stub-matched MZM*

As demonstrated in [11], a stub-matched MZM electrode can be approximated using an equivalent transmission line circuit. The transmission line equivalent circuit corresponding to an open-ended electrode configuration is shown in Figure 10.

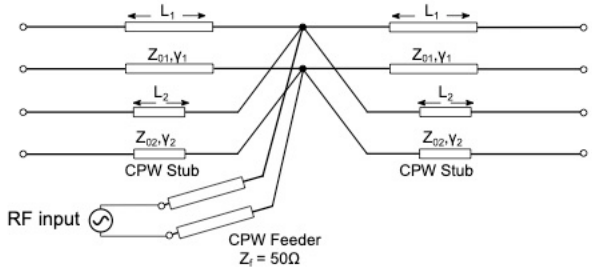


*Figure 10 Equivalent transmission line model*

The co-planar transmission lines for the stubs were designed with Keysight Advanced Design System (ADS). The phase-shifter transmission line is a co-planar waveguide of which one of the slots is loaded with the pn-doped silicon waveguide and was taken from the iSiPP25G PDK. The transmission line parameters of the phase-shifter were determined using an electro-magnetic field-solver simulation. The structure was designed to have an input impedance of 50 Ohm for a frequency of 28 GHz. The resulting length for the phase-shifter is 1.6 mm ($L_1$ = 0.8 mm), resulting in a static Vpi of 6.3 V and a phase-shifter insertion loss of 5 dB. Matching was achieved using stubs of L2= 0.8 mm long. A microscope image of the fabricated modulator is shown in Figure 11.

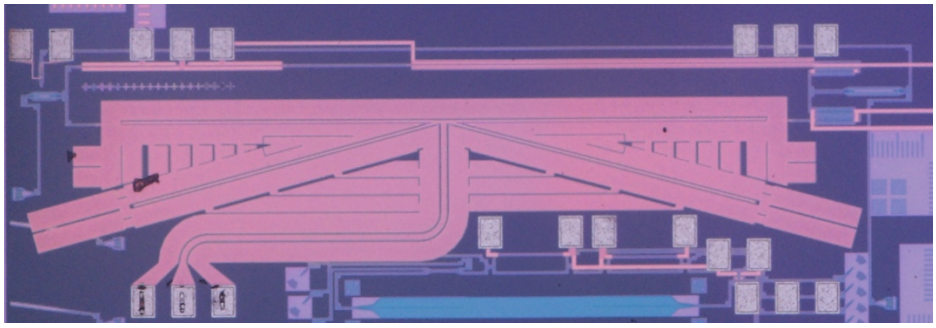

*Figure 11 Microscope image of the resonant stub-matched MZM*

To investigate the impedance matching we performed a S11 measurement of the structure using a Keysight PNA-X vector network analyzer. In Figure 12(a) the return loss is shown as function of the frequency. A resonance in the reflection coefficient is seen between 15 and 25 GHz, which deviates from the design target of 28 GHz. Furthermore, the 3 dB bandwidth of the S11 resonance is relatively broad (8 GHz) resulting in a low Q-factor (˜3). Finally we measured the S21 of the phase-shifter placed in a MZI structure, the result is shown in Figure 12(b). Due to the strong roll-off of the modulator as a whole, it is difficult to distinguish the resonant behavior in the S21 graph.

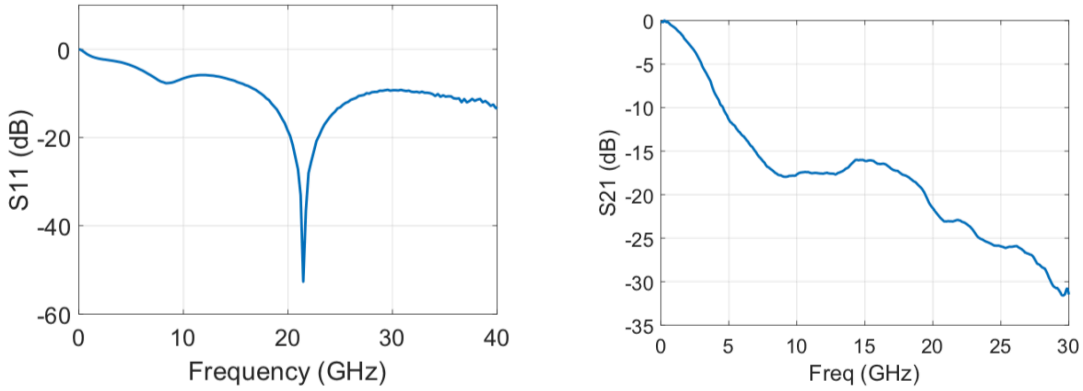


*Figure 12 (a) S11 and (b) S21 response for the stub-matched MZM*

## 3. CONCLUSIONS AND OUTLOOK

We demonstrated that two monolithically integrated InP-based lasers integrated on a single chip can be locked to the same optical cavity using the PDH frequency locking technique. The PDH is implemented with a single control loop and voltage control electro-optic tuning therefore avoiding significant heat dissipation. The frequency difference of the stabilized lasers can be discretely tuned at multiples of the FSR of the external optical cavity and used for RF signal generation. We presented generated tones at 12.436 GHz, 24.8735 GHz and 40.4194 GHz, limited only by the bandwidth of the photodetector, with FWHM <40 kHz. The SSB phase noise is lower than 50 dBc/Hz for all frequency offsets.

The obtained SSB phase noise of the RF signal is not as good as state of the art oscillators up to several tens of GHz frequency at the moment. The phase noise can be improved however in two ways. At low offset frequencies (couple of MHz) further suppression of the laser frequency noise can be achieved with improvement of the PDH locking system with higher gain. At high offset frequencies, lasers with lower intrinsic linewidth should be used since implementation of PDH locking with such control bandwidths is very challenging.

Despite the SSB phase noise not being better than the state-of-the-art this technique has several advantages. The tuning range can be extended by more than an order of magnitude by using lasers realised in the same technology. Such tuneable lasers can be tuned over tens of nm (several THz) and can be stabilized in the same way as shown in this report. Therefore discrete tuning from microwave to THz frequencies can be enabled. In the same technology we have demonstrated that widely tuneable lasers can have roughly the same frequency noise level independent of their lasing wavelength. The implementation of this technique with such lasers would yield virtually quality of the generated signal

independent of its frequency. Furthermore, the long-term drift of the generated tone depends on the variations of the FSR of the cavity which are much smaller that the actual drift of the resonant frequencies. Finally, further integration of the system can be pursued such as combining the two laser outputs using an MMI and mixing them on an integrated photo-detector and using available modulators such as Mach-Zehnder or electro-absorption modulators.

On the Si Photonics modulator side, we demonstrated two types of Mach-Zehnder modulators for 30 GHz operation (traveling wave MZM and a stub-matched resonant MZM). 30GHz bandwidth is demonstrated for the traveling wave devices and the concept of the stub-matching is demonstrated, although the matching occurs at a slightly lower frequency because of the inaccurate model for the transmission lines on the silicon photonic circuit. By properly calibrating the transmission line model 30GHz stub-matching can be obtained.

## REFERENCES


[1] A. J. Seeds: Microwave Photonics, *IEEE Trans. Microwave Theory Tech.,* vol. 50, no. 3, pp. 877-887, Mar. 2002.

[2] G. Carpintero et al.: Microwave Photonic Integrated Circuits for Millimetre-Wave Wireless Communications, *Journal of Lightwave Technology*, vol. 32, np. 20, pp. 3495-3501, Oct, 2014.

[3] K. Balakier et al.: Monolithically Integrated Optical Phase Lock Loop for Microwave Photonics, *Journal of Lightwave Technology*, vol. 32, no. 20, pp. 3893-3900, Oct. 2014.

[4] Bente E.A.J.M et al.: Mode-locked lasers in InP photonic integrated circuits, in *Proc. SPIE,* vol. 10123, Feb., 2017

[5] L. Maleki: The optoelectronic oscillator, *Nature Photon.*, vol. 5, pp. 728–730, Dec. 2011.

[6] L. M. Augustin et al.: InP-Based Generic Foundry Platform for Photonic Integrated Circuits, *IEEE Journal of Selected Topics in Quantum Electronics,* vol. 24, no. 1, pp. 1-10, 2018.

[7] R. W. P. Drever, J. L. Hall, F. V. Kowalski, J. Hough, G. M. Ford, A. J. Munley and H. Ward, "Laser phase and frequency stabilization using an optical resonator," *Applied Physics B*, vol. 31, no 12, pp. 97-105, Jun. 1983.

[8] S. Andreou, K. A. Williams, E.A.J.M. Bente: An InP-based DBR laser with an intra-cavity ring resonator with 130 kHz linewidth and 65 dB SMSR, in *Proc. IEEE ISLC 2018,* Sept., 2018, paper TuD2.

[9] A. Samani, M. Chagnon, D. Patel, V. Veerasubramanian, S. Ghosh, M. Osman, Q. Zhong, and D. V. Plant. A Low-Voltage 35-GHz Silicon Photonic Modulator-Enabled 112-Gb/s Transmission System. IEEE Photonics Journal, 7(3):1–13, jun 2015

[10] R. Krahenbuhl and M. Howerton. Investigations on short-path-length high-speed optical modulators in LiNbO with resonant-type electrodes. Journal of Lightwave Technology, 19(9):1287–1297, 2001.

[11] S. Oikawa, T. Kawanishi, K. Higuma, Y. Matsuo, and M. Izutsu. Double-stub structure for resonant-type optical modulators using 20- μm-thick electrode. IEEE Photonics Technology Letters, 15(2):221–223, feb 2003.